Membrane Cholesterol Modulates Oligomeric Status and Peptide-membrane Interaction of Severe Acute Respiratory Syndrome Coronavirus Fusion Peptide

Geetanjali Meher, Surajit Bhattacharjya, and Hirak Chakraborty

Just Accepted

Membrane Cholesterol Modulates Oligomeric Status and Peptide-Membrane Interaction of Severe Acute Respiratory Syndrome Coronavirus Fusion Peptide

Geetanjali Meher,[†] Surajit Bhattacharjya[§]* and Hirak Chakraborty[†,¶]*

[†]School of Chemistry, Sambalpur University, Jyoti Vihar, Burla, Odisha 768 019, India

[¶]Centre of Excellence in Natural Products and Therapeutics, Sambalpur University, Jyoti Vihar,

Burla, Odisha 768 019, India

[§] School of Biological Sciences, Nanyang Technological University, 60 Nanyang Drive, Singapore

637551

*Address correspondence to Hirak Chakraborty, E-mail: hirak@suniv.ac.in or

hirakchakraborty@gmail.com, Phone: +91-8008716419 or Surajit Bhattacharjya, Email:

surajit@ntu.edu.sg. Fax: 65-6791-3856.

ABSTRACT: The N-terminal fusion peptide (residues 770–788) of S2 glycoprotein of the severe acute respiratory syndrome corona virus (SARS-CoV), exposed upon receptor binding, is crucial for virus entry into the host cell. The fusion peptide alters the membrane organization and dynamics of the host membrane to facilitate membrane fusion. Generally, the effect of fusion peptide on the membrane is sensitive to the lipid composition of target membranes. In this present work, we have utilized steady state and time-resolved fluorescence spectroscopy in tandem with circular dichroism spectroscopy to elucidate the binding, oligomeric status, secondary structure of the fusion peptide and its impact on the depth-dependent membrane organization and dynamics. We have used depth-dependent fluorescence probes, 1,6-diphenyl-1,3,5-hexatriene (DPH) and its trimethylammonium derivative (TMA-DPH), to evaluate the effect of the peptide-binding along the bilayer normal. We have exploited the energy transfer efficiency of tryptophan between TMA-DPH and DPH to determine the relative location of the solitary tryptophan present in the membrane-bound fusion peptide. We have further evaluated the effect of membrane cholesterol on the binding and organization of the peptide and the impact of peptide binding on the depth-dependent physical properties of the membrane at various cholesterol concentrations. Our results clearly demonstrate that the membrane cholesterol alters the oligomeric status of the membrane-bound peptide and the effect of peptide-binding on the depth-dependent membrane organization and dynamics. The role of cholesterol is important as the eukaryotic host cells contain good amount of cholesterol that might be important for the entry of pathogenic viruses.

INTRODUCTION

Severe Acute Respiratory Syndrome (SARS) is an emerging form of pneumonia caused by SARS-CoVs.[1-3] Coronaviruses are enveloped, positive-stranded RNA viruses with the largest genome, and are characterized by 3–4 envelope proteins embedded on their surface.[4] Like other enveloped viruses, coronavirus enters the host cell via fusion of the lipid bilayer of viral envelope with the host cell membrane. The surface glycoprotein S of SARS-CoV binds to the host cell receptors angiotensin-converting enzyme (ACE2) and CD209L to induce membrane fusion.[5-6] Recent studies have shown SARS-CoV to enter the cell via receptor-mediated endocytosis.[2, 7] The binding of S1 subunit of S protein with the receptor leads to cleavage of the protein, thereby initiating conformational changes in the other subunit, S2.[8] While the S1 subunit binds to the cell surface receptor, S2 subunit induces fusion between the virus and target cell membranes.[8-10] The conformational change in S2 subunit exposes the N-terminal fusion peptide, which plays an instrumental role in the fusion process.[9] The S2 protein contains heptad repeats, HR1 and HR2, and a transmembrane region at the C-terminus, in addition to the membrane-active fusion peptide (FP), internal fusion peptide (IFP), and pre-transmembrane peptide (PTM). HR1 and HR2 regions are known to form antiparallel oligomers.[11-14] Atomic resolution structure of HR1 and HR2 complex had shown the formation of a six-helix bundle, which is an important characteristic of class I fusion peptide.[15-18] However, there has been no information yet regarding the oligomeric status of fusion peptide and its implication in membrane fusion. Generally, fusion peptide is a stretch of 20–25 amino acids located at the N-terminus of class I viral fusion protein. Its interaction with the host cell has been extensively shown to be the first step of fusion between virus and host cells.[19] An alternative mechanism suggests the requirement of both receptor-mediated endocytosis and pH-driven conformational change for the fusion.[20-21] In that case, SARS-CoV has been proposed to be

internalized in the cell through endocytosis, followed by its exposure to a low-pH environment, thus leading to the proteolytic cleavage of S1 and S2 domains. Moreover, cholesterol- and sphingolipid-rich raft microdomains have been also shown to be involved in virus entry.[21-22]

In general, membrane composition plays a key role in the behavior of fusion protein and its effect on membrane fusion by modulating the organization and dynamics of both the membrane as well as the fusion protein.[23-24] The fusion peptide of SARS-CoV has been shown to preferentially bind to membrane containing negatively charged lipids owing to +2 formal charges on the peptide at physiological pH.[3] Insertion of fusion peptide into the membrane reduces the dipole potential of negatively charged membranes, the effect being more pronounced in presence of cholesterol.[25] In addition, SARS-CoV fusion peptide promotes water penetration in the hydrophobic region of DMPC and DMPG membranes, remarkably more in the latter.[3] Lipid composition also has significant impact on the rate of lipid mixing. Large unilamellar vesicles (LUVs) containing cholesterol undergo faster lipid mixing than the membranes devoid of cholesterol.[3, 25] Cholesterol is known to have unique effect on the fusion peptide structure, membrane interaction, and fusion. The SARS-CoV fusion peptide has been recently shown to assume a bent helical conformation ('V-shaped') around residues 5–18, and largely non-helical or extended conformations around the N-terminal residues W2–T4 in DPC micelles.[26-27] However, it has a propensity to adopt β-sheet structure upon interaction with lipid membranes.[28] FTIR spectra of SARS-CoV fusion peptide had shown extended β-strands with strong intermolecular interactions in presence of phospholipids.[3]

In the current study, we have investigated the structure and oligomeric status of SARS-CoV fusion peptide, and its effect on the organization and dynamics of POPC/POPG membranes, with varying amounts of cholesterol. Our results revealed the effect of cholesterol on structure and oligomeric status of the peptide. We have further evaluated the effect of fusion peptide on membrane

organization and dynamics at various membrane compositions. We have extensively utilized steady

state and time-resolved fluorescence properties of tryptophan in the SARS-CoV fusion peptide and

of two depth-dependent extrinsic fluorophores, DPH and TMA-DPH, in order to elucidate the

oligomeric status of the peptide and its effect on depth-dependent membrane organization and

dynamics. We have determined secondary structure of the fusion peptide in different membranes

using circular dichroism spectroscopy. Our results demonstrated the binding affinity of SARS-CoV

fusion peptide to increase with increasing membrane cholesterol. Moreover, the fusion peptide

demonstrated concentration-dependent oligomerization in cholesterol-containing membrane, with

high oligomerization propensity in the membrane containing 20 mol% of cholesterol. The impact

of peptide binding on membrane properties depends on the lipid composition of the membrane and

oligomeric status of the peptide. The peptide assumes majorly unstructured conformation, with

approximately 20% β-sheet and 10% α-helical conformation in the membrane of different lipid

compositions. The fusion peptide of SARS-CoV mainly partitions in the interfacial region of

POPC/POPG (80/20 mol%) and POPC/POPG/Chol (60/20/20 mol%) membranes, and penetrates in

the hydrophobic region of the membrane in POPC/POPG/Chol (70/20/10 mol%) membranes. Taken

together, our present work provides a detailed overview of the structure, oligomeric status, and

penetration depth of the SARS-CoV fusion peptide in membranes containing varying cholesterol

concentration, and its effect on the organization and dynamics of the membrane.

MATERIALS AND METHODS

   Materials. 1-Paimitoyl-2-oleoyl-*sn*-glycero-3-phosphocholine (POPC), cholesterol (Chol),

and 1-paimitoyl-2-oleoyl-*sn*-glycero-3-phosphoglycerol (sodium salt) (POPG) were purchased from

Avanti   Polar   Lipids   (Alabaster,   AL).   1,6-Diphenyl-1,3,5-hexatriene   (DPH)   and

trimethylammonium derivative of DPH (TMA-DPH) were purchased from Molecular Probes/Invitrogen (Eugene, OR). Sodium dihydrogen phosphate dihydrate and disodium hydrogen phosphate were obtained from Merck, India. Spectroscopic grade DMSO was purchased from Spectrochem (India). All other chemicals used in the study were of the highest available purity. Water was purified in a Millipore (Bedford, MA) Milli-Q water purification system.

Peptide Synthesis. The fusion peptide of SARS-CoV was purchased commercially from GL-Biochem (China) with purity of > 98%. The peptide sequence was MWKTPTLKYFGGFNFSQIL without any modification in the N- and C-terminals. Small aliquots of peptide stock solutions, prepared in DMSO, were added to the vesicle suspensions. The amount of DMSO was always less than 1% (v/v), such that it had no detectable effect on either fusion or membrane structure.

Preparation of Vesicles. Large unilamellar vesicles (LUVs; diameter approximately 100 nm) were prepared from a mixture of POPC/POPG (80/20 mol%) or POPC/POPG/Chol (70/20/10 mol% and 60/20/20 mol%); the concentration of lipid was kept constant at 200 µM in all experiments. We used DPH to probe the hydrophobic region of the membrane and TMA-DPH to probe the interfacial region. The concentration of DPH or TMA-DPH was kept constant at 1 µM (1 mol% with respect to lipid concentration) to minimize the probe-induced alteration of membrane structure. The lipid was dissolved in chloroform and air dried to make a thin film. The film was kept overnight in a vacuum desiccator to ensure complete removal of chloroform. The lipid film was hydrated (swelled) by adding 10 mM phosphate buffer, pH 7.4. The sample was vortexed for 1h for uniform dispersion of lipids. LUVs with a diameter of 100 nm were prepared by extrusion technique, using Avanti Mini-Extruder (Alabester, AL) as described previously.[29] Background samples were prepared the same way except that the peptides were omitted.

Small aliquots of peptides and probes were added from their respective stock solutions, prepared in DMSO, to prepare the working solutions. DMSO content was always less than 1% (v/v), since such a small quantity of DMSO had no detectable effect on membrane structure and its interaction with peptide .[30]

Steady State Fluorescence Measurements. Steady state fluorescence measurements were carried out in Hitachi F-7000 (Japan) spectrofluorometer using quartz cuvettes of - 1 cm path length. Tryptophan was excited at 295 nm and its fluorescence monitored from 310 to 450 nm. Excitation and emission slits with a nominal band pass of 5 nm were used for all measurements. Background (peptide-free) intensities of samples were subtracted from each sample spectrum to eliminate the contribution of solvent Raman peak and other scattering artefacts.

Fluorescence anisotropy measurements of DPH and TMA-DPH were performed using the same instrument, fixing excitation wavelength at 360 nm and monitoring emission at 428 nm. Excitation and emission slits with a nominal band pass of 5 nm were used for this set of experiments. Fluorescence anisotropy measurement of Tryptophan was performed similarly, with excitation wavelength at 295 nm and emission at 350 nm. Excitation and emission slits with a nominal band pass of 10 nm were used for the measurement of tryptophan fluorescence anisotropy. Background (peptide-free) intensities of samples were subtracted from each sample spectrum to eliminate the contribution of solvent Raman peak and other scattering artefacts in case of fluorescence anisotropy of Tryptophan. Anisotropy values were calculated using the following equation:[31]

$$r = \frac{I_{VV} - G \times I_{VH}}{I_{VV} + 2G \times I_{VH}} \qquad (1)$$

7

where G = I_{HV}/I_{HH}, (grating correction or G-factor), I_{VV} and I_{VH} are the measured fluorescence intensities with excitation polarizer vertically oriented and emission polarizer vertically and horizontally oriented, respectively.

Time-resolved Fluorescence Measurements. Fluorescence lifetimes were calculated from time-resolved fluorescence intensity decays using the IBH 5000F Nano LED equipment (Horiba Jobin Yvon, Edison, NJ) and Data Station software in the time-correlated single photon counting (TCSPC) mode. A pulsed light-emitting diode (LED) was used as the excitation source. This LED generates optical pulse at 290/338 nm, with pulse duration 1.2 ns, and is run at 1 MHz repetition rate. The LED profile (instrument response function) was measured at the excitation wavelength using Ludox (colloidal silica) as the scatterer. To optimize the signal-to-noise ratio, 10,000 photon counts were collected in the peak channel. All experiments were performed using emission slits of band pass 16 nm. The sample and the scatterer were alternated after every 10% acquisition to ensure compensation for shape and timing drifts occurring during data collection. This arrangement also prevents prolonged exposure of the sample to the excitation beam, thereby avoiding any possible photo damage of the fluorophore. Data were stored and analyzed using DAS 6.2 software (Horiba Jobin Yvon, Edison, NJ). Fluorescence intensity decay curves were deconvoluted with the instrument response function and analyzed as a sum of exponential terms:

$$F(t) = \sum_i^n \alpha_i exp(-t/\tau_i)$$

A considerable plot was obtained with random deviation about zero with a minimum $\chi 2$ value of 1.2 or less. Intensity averaged mean lifetimes τ_{avg} for tri-exponential decays of fluorescence were calculated from the decay times and pre-exponential factors using the following equation:[31]

$$\tau_{avg} = \frac{\sum \alpha_i \tau_i^2}{\sum \alpha_i \tau_i} \tag{2}$$

where α_i is the fraction that shows τ_i lifetime.

Circular Dichroic Spectroscopy. Circular Dichroic (CD) spectra of SARS-CoV fusion peptide (7.5 µM) in three different membranes were measured in a Jasco 1500 (Japan) Spectrophotometer. The spectra were recorded in the wavelength range of 190–260 nm using cylindrical quartz cuvette of 4-mm path length. The spectra were scanned in 0.5 nm wavelength increments, with band width of 2 nm and scan rate of 50 nm/min. All circular dichroic spectra were averages of at least 3 consecutive scans. The background spectrum (without protein) was recorded with the same parameters and was subtracted from each sample spectrum. All CD measurements were carried out in 5 mM phosphate buffer, pH 7.4. The ellipticity values obtained from the instrument were converted into molar ellipticity using the following equation:

$$[\theta] = \frac{<\theta>_{degree}}{10 bnc} \tag{7}$$

where, '$<\theta>$' is the ellipticity measured by CD spectroscopy, 'b' is the path length in cm, 'n' is the number of amino acid residues present in the fluorophore, and 'c' is the concentration of protein solution in moles litre^{-1}. The lipid and peptide concentrations used in the CD measurements were 100 µM and 7.5 µM, respectively. The CD spectra were analyzed using Dichroweb for the evaluation of secondary structural components. [32-33]

Fluorescence Resonance Energy Transfer Efficiency Measurements. The penetration depth of SARS-CoV fusion peptide was measured in three different membranes by monitoring the ratio of fluorescence resonance energy transfer (FRET) efficiency of tryptophan between TMA-DPH and DPH. DPH and TMA-DPH are known to locate at two different regions of the bilayer, DPH being at an average distance of approximately 7.8 Å from the centre of the bilayer while TMA-DPH locates at the interfacial region, owing to its polar trimethylammonium group, with an average distance of approximately 10.9 Å from the centre of the bilayer.[34] We have utilized the distance

dependence of FRET efficiency,[35] and measured the same between tryptophan and TMA-DPH, and tryptophan and DPH, separately. FRET of the peptide in presence of DPH and TMA-DPH was monitored by exciting its tryptophan at 295 nm and observing emission at 346 nm. Background intensities of the samples were subtracted from each sample spectrum to eliminate the contribution of solvent Raman peak and other scattering artefacts. Fluorescence intensity of the donor (F_D, tryptophan) was measured in absence and presence of the acceptor (F_{DA}, TMA-DPH or DPH), and FRET efficiency was calculated using the following equation:[31]

$$E_T = 1 - \left(\frac{F_{DA}}{F_D}\right) \tag{8}$$

Subsequently, we calculated the ratio of FRET efficiency of tryptophan between TMA-DPH and DPH (E_T(TMA-DPH)/E_T(DPH)), and the location of tryptophan was speculated therefrom; higher ratio indicated close proximity of tryptophan to TMA-DPH (shallow penetration) while lower ratio indicated its closeness to DPH (deeper penetration).

RESULTS

Fusion peptide is known to interact with the host cell membrane in order to induce fusion; the efficiency of membrane fusion depends on lipid composition of the host cell membrane.[24] Therefore, here, we have studied the interaction of SARS-CoV fusion peptide with POPC/POPG membranes in presence of varying concentrations of cholesterol. We have extensively utilized steady state and time-resolved fluorescence spectroscopy in tandem with circular dichroism spectroscopy to elucidate the binding efficiency, oligomeric status, and structure of the fusion peptide, along with its impact on the organization and dynamics of membranes with different lipid compositions.

Membrane Cholesterol Promoted the Binding of Fusion Peptide. The binding affinity of SARS-CoV fusion peptide in different membranes was evaluated by monitoring the change in

tryptophan (Trp) fluorescence intensity with increasing concentration of lipid. Plots of normalized

fluorescence intensity as a function of lipid concentration are shown in Figure 1 (A and B). The

enhancement of Trp fluorescence intensity with increasing concentration of POPC/POPG (80/20

mol%) and POPC/POPG/Chol (70/20/10 mol%) membranes indicated partitioning of the peptide in

the lipid membranes. Binding affinity of the peptide was analyzed using classical Langmuir model

for adsorption of ligand to multiple, equivalent, and non-interacting surface sites, as described

earlier.[36-37] Tryptophan fluorescence intensity was found to decrease with increasing concentration

of POPC/POPG/Chol (60/20/20 mol%) membranes, although the nature of reduction of fluorescence

intensity resembled the binding isotherm; the binding affinity was calculated using the model

described above. Decrease in fluorescence intensity with peptide binding to the membrane could be

due to the presence of a quencher amino acid, such as phenylalanine, in the vicinity of tryptophan.[38]

The unique appearance of quencher amino acid near tryptophan, in presence of POPC/POPG/Chol

(60/20/20 mol%) membranes, might be due to either conformational change of the peptide or its

oligomerization in the membrane containing 20 mol% of cholesterol. Interestingly, binding affinity

of the peptide increased with increasing concentration of cholesterol in the membrane. The K_d

values of SARS-CoV fusion peptide in different membranes are shown in Table-1.
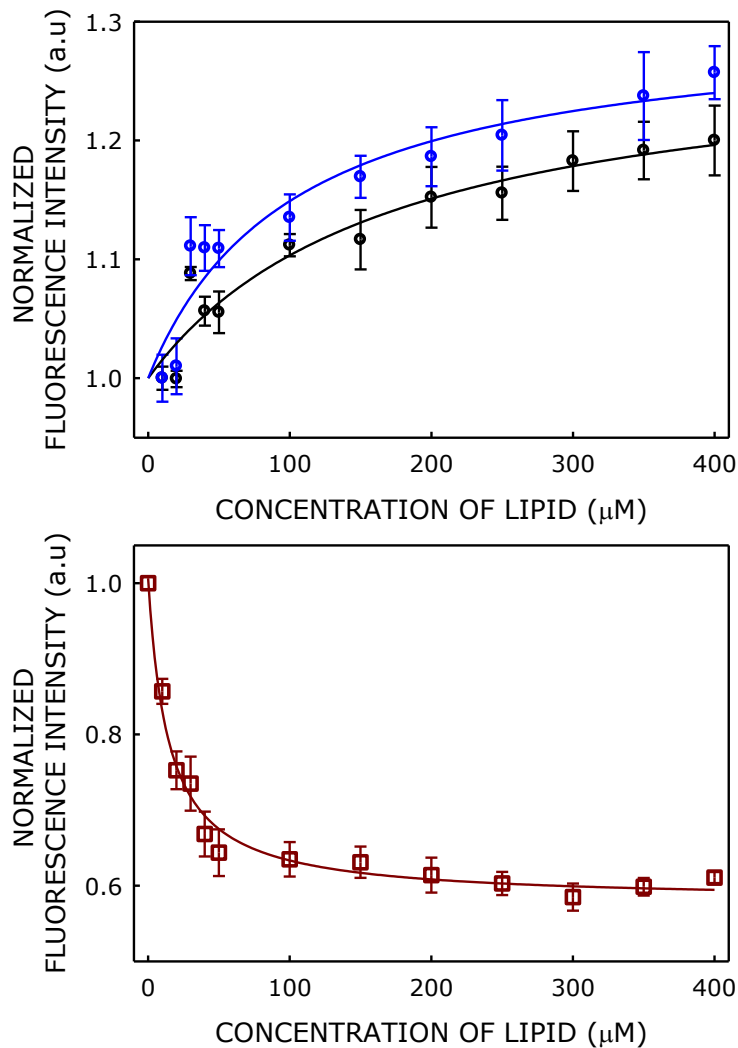
Figure 1. Plot of normalized fluorescence intensity of tryptophan with varying concentration of (A)

POPC/POPG (80/20 mol%) (black, o), POPC/POPG/Chol (70/20/10 mol%) (blue, Δ) and (B)

POPC/POPG/Chol (60/20/20 mol%) (red, □) membranes. All experiments were carried out in a 10

mM phosphate buffer of pH 7.4 at 25 °C. The concentration of peptide was kept constant at 2 μM

and the emission was monitored at 338 nm by exciting at 295 nm. See the Materials and Methods

section for more details.

Table-1. Binding Affinity (K_d) of SARS-CoV Fusion Peptide in Different Membranes

Membrane composition	K_d (µM)
POPC/POPG (80/20 mol%)	171.2
POPC/POPG/Chol (70/20/10 mol%)	102.2
POPC/POPG/Chol (60/20/20 mol%)	14.8

Membrane Cholesterol Induced Oligomerization of Fusion Peptide. Generally, fluorescence anisotropy is used to investigate rotational flexibility around the fluorophore in any microheterogeneous environment. The fluorescence anisotropy of tryptophan was measured as a function of peptide concentration to evaluate its rotational flexibility in different membranes. The fluorescence anisotropies as a function of peptide concentration, in three different membranes, are shown in Figure 2. Fluorescence anisotropy of tryptophan did not show any appreciable change with increasing concentration of the peptide in POPC/POPG (80/20 mol%) membranes, whereas it decreased with peptide concentration in cholesterol-containing membranes. However, this decrease was initiated at much lower peptide concentrations when the membrane contained 20 mol% cholesterol. Moreover, the change in fluorescence anisotropy was much sharper in presence of 20 mol% cholesterol compared to that in presence of 10 mol% cholesterol.

Fluorescence anisotropy is known to decrease due to the occurrence of Homo-FRET.[39] Homo-FRET is an energy transfer process between two or more identical fluorophores if the fluorophore demonstrates relatively smaller Stokes' shift.[40] The transfer of energy from one dipole to another in different orientation always leads to depolarization of the emitted light, thereby reducing the fluorescence anisotropy value.[41] Therefore, decrease in tryptophan fluorescence anisotropy with increasing concentration of the peptide in cholesterol-containing membranes indicated oligomerization of SARS-CoV fusion peptide in the membrane. The fluorescence anisotropy results demonstrated the propensity of oligomerization to be much higher in the

membrane containing 20 mol% cholesterol (oligomerization onsets in L/P ratio >100) than in the membrane containing 10 mol% cholesterol (oligomerization onsets in L/P ratio > 40). Our results shed light on the vital issue of protein-induced membrane fusion, where oligomerization of fusion protein is hypothesized to lead to the formation of six-helix bundle, thereby bringing the host membrane close to the virus membrane. The crystal structure of gp41, devoid of fusion peptide and transmembrane domain, clearly validated the claim of oligomerization and six-helix bundle formation.[42] However, evidence elucidating the oligomerization of fusion peptide in membrane is still lacking. The chemically crosslinked trimer of gp41 fusion peptide showed enhanced membrane fusion, thereby supporting oligomerization of gp41 fusion peptide in membranes.[43] Although Dimitrov's group had shown the SARS-CoV S glycoprotein without the fusion peptide sequence to oligomerize in the membrane,[44] there is no evidence yet in support of oligomerization of the fusion peptide.
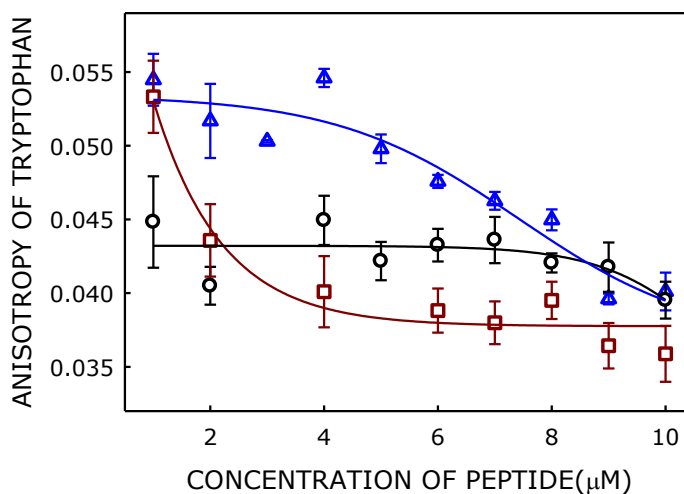
Figure 2. Change in average fluorescence anisotropy of tryptophan with varying concentration of POPC/POPG (80/20 mol%) (black, o), POPC/POPG/Chol (70/20/10 mol%) (blue, Δ) and POPC/POPG/Chol (60/20/20 mol%) (red, □) membranes. All experiments were carried out in a 10 mM phosphate buffer of pH 7.4 at 25 ℃. The concentration of lipid was kept constant at 200 μM

and the emission was monitored at 350 nm by exciting at 295 nm. See the Materials and Methods section for more details.

Cholesterol Promoted Fusion Peptide-induced Hydrophobic Tail Ordering in the Membrane. DPH is a rod-like molecule located in the hydrophobic region of the membrane with an average distance of approximately 7.8 Å from the bilayer center.[34] The rotational flexibility of DPH in POPC/POPG and POPC/POPG/Chol membranes, with varying peptide concentrations, was monitored by measuring fluorescence anisotropy (r) of DPH. The fluorescence anisotropy value increased with increase in peptide concentration, in absence and presence of cholesterol in POPC/POPG membranes, as shown in Figure 3. However, the change of fluorescence anisotropy in the cholesterol-free membrane (POPC/POPG; 80/20 mol%) geared up at higher peptide concentrations, thereby indicating less effect of peptide in ordering the hydrophobic region up to an L/P ratio of 40 ($\Delta r = 0.003$). The peptide was found to be mainly monomeric in this lipid composition; therefore, our result indicated the monomeric peptide to have minimal effect on the hydrophobic order in the membrane without cholesterol. Fluorescence anisotropy increases significantly in the membrane containing POPC/POPG/Chol (70/20/10 mol%) at the initial concentrations of fusion peptide, and reaches a plateau in presence of 3 µM fusion peptide. Change in fluorescence anisotropy (Δr) of DPH at a lipid-to-peptide ratio of 40 was approximately 0.013, which was much higher than that in the membranes without cholesterol at the same lipid-to-peptide ratio. The fusion peptide is monomeric in POPC/POPG/Chol (70/20/10 mol%) at a lipid-to-peptide ratio of 40, thereby suggesting that the peptide penetrated deeper in the membrane when the latter contained 10 mol% cholesterol. Measurement of penetration depth of the peptide might help to justify our claim of deeper penetration of the peptide in POPC/POPG/Chol (70/20/10 mol%) membranes. The membrane containing 20 mol% cholesterol showed significant increase in the peptide-dependent change in the fluorescence anisotropy of DPH. Interestingly, in the POPC/POPG/Chol (60/20/20 mol%) membrane, the anisotropy value saturated at a lower concentration of the peptide (1 µM). Since the peptide is oligomeric in nature at this lipid

composition, change in fluorescence anisotropy ($\Delta r = 0.008$ at lipid to peptide ratio 40) of DPH

could either be due to oligomerization of the peptide or deeper penetration of the oligomeric species
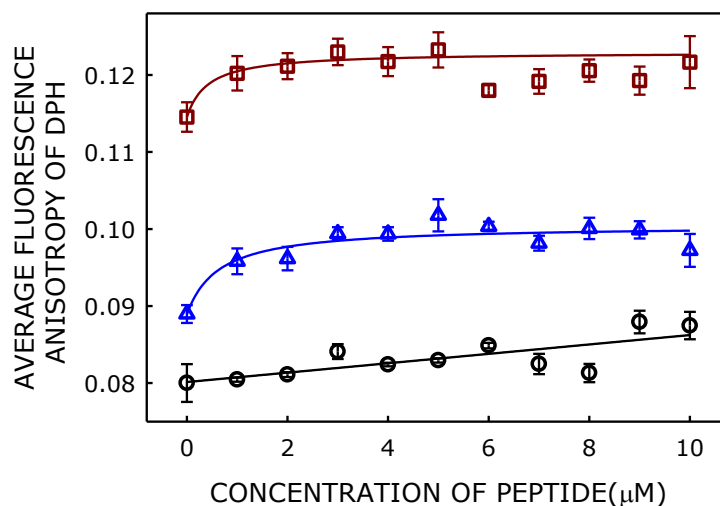
in the membrane containing 20 mol% cholesterol.

Figure 3. Plot of average fluorescence anisotropy of DPH with varying concentration of SARS-CoV

fusion peptide in POPC/POPG (80/20 mol%) (black, o), POPC/POPG/Chol (70/20/10 mol%) (blue,

Δ) and POPC/POPG/Chol (60/20/20 mol%) (red, □) membranes. All experiments were carried out

in a 10 mM phosphate buffer of pH 7.4 at 25 ℃. The concentration of lipid and DPH were kept

constant at 200 μM and 1μM, respectively. The emission was monitored at 428 nm by exciting at

360 nm. See the Materials and Methods section for more details.

Fusion Peptide Did Not Alter the Polarity of Hydrophobic Region. Fluorescence lifetime

was used to determine the polarity of neighboring microenvironment of the probe. We have utilized

the change in fluorescence lifetime of DPH in membranes to monitor the change in polarity (water

penetration) of the hydrophobic region of the membrane with increasing concentration of the SARS-

CoV fusion peptide, as shown in Figure 4. Although no significant change in fluorescence lifetime

of DPH was seen in presence of the fusion peptide in cholesterol-containing membranes, the peptide

did alter polarity of the hydrophobic region of the membrane to a small extent (change in fluorescence lifetime of DPH is approximately 100 ps) at higher peptide concentrations. Taken together, our results indicated the SARS-CoV fusion peptide do not have much impact on the hydrophobic polarity of membranes having variable lipid compositions. Therefore, it is clear that neither the oligomeric status nor lipid composition has any SARS-CoV fusion peptide-induced effect on hydrophobic polarity of the membrane.
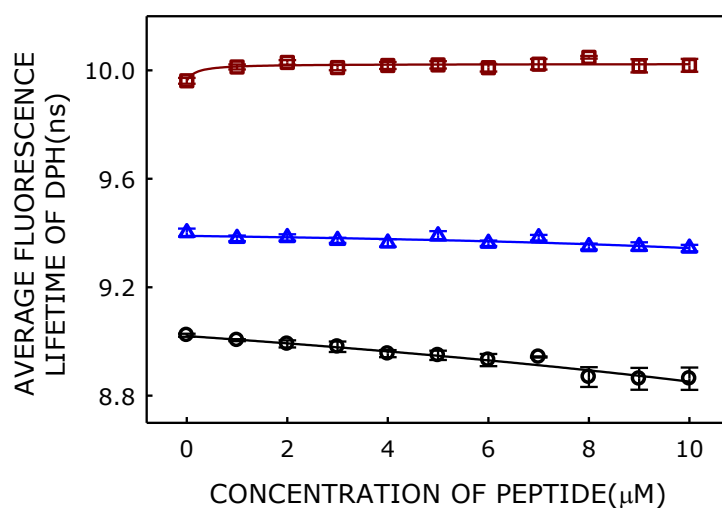
Figure 4. Plot of mean fluorescence lifetime of DPH in varying concentration of SARS-CoV fusion peptide in in POPC/POPG (80/20 mol%) (black, o), POPC/POPG/Chol (70/20/10 mol%) (blue, Δ) and POPC/POPG/Chol (60/20/20 mol%) (red, □) membranes. All experiments were carried out in a 10 mM phosphate buffer of pH 7.4 at 25 ℃. The concentration of lipid and TMA-DPH were kept constant at 200 μM and 1 μM, respectively. The emission was monitored at 428 nm by exciting at 338 nm. See the Materials and Methods section for more details.

Fusion Peptide Oligomers Disrupted Interfacial Ordering of the Membrane. TMA-DPH is known to be located at the interfacial region of the bilayer with an average distance of 10.9 Å from

the bilayer centre.[34] Rotational flexibility of the interfacial region could be monitored by measuring

the fluorescence anisotropy of TMA-DPH. Fluorescence anisotropy of TMA-DPH, in presence of

SARS-CoV fusion peptide, in different membranes is shown in Figure 5. The anisotropy values did

not change in presence of various concentrations of the peptide in POPC/POPG (80/20 mol%) and

POPC/POPG/Chol (70/20/10 mol%) membranes. However, addition of fusion peptide remarkably

reduced the fluorescence anisotropy of TMA-DPH in POPC/POPG/Chol (60/20/20 mol%)

membranes. Our results suggested the oligomeric peptide to be highly disruptive toward the

interfacial order of the membrane, which is indicative of the interfacial localization of oligomeric

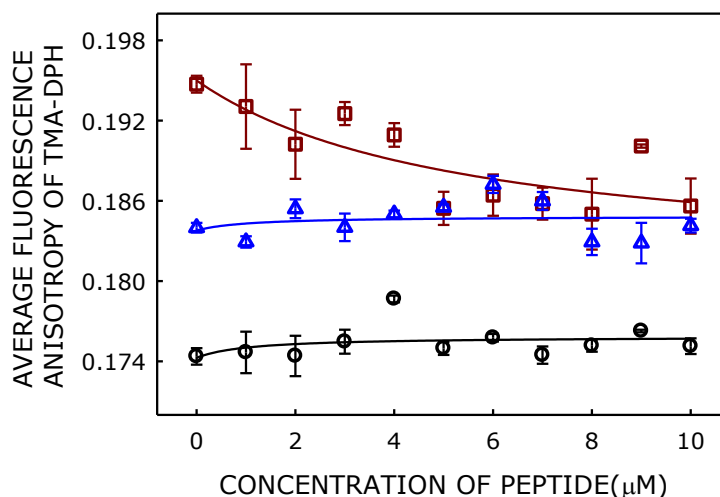forms in the 20 mol%-cholesterol containing membranes.

Figure 5. Plot of average fluorescence anisotropy of TMA-DPH in varying concentration of SARS-

CoV fusion peptide in in POPC/POPG (80/20 mol%) (black, o), POPC/POPG/Chol (70/20/10

mol%) (blue, Δ) and POPC/POPG/Chol (60/20/20 mol%) (red, □) membranes. All experiments

were carried out in a 10 mM phosphate buffer of pH 7.4 at 25 °C. The concentration of lipid and

TMA-DPH were kept constant at 200 μM and 1μM, respectively. The emission was monitored at

428 nm by exciting at 360 nm. See the Materials and Methods section for more details.

Fusion Peptide Had Minimal Effect on Polarity of the Membrane Interfacial Region.
Polarity around the interfacial probe, TMA-DPH, was monitored at varying concentrations of peptide in three different membranes by measuring TMA-DPH lifetime, and the results are shown in Figure 6. The fusion peptide did not show any significant change in peptide-dependent polarity of the interfacial region of membranes in all three lipid compositions. Nonetheless, there was an appreciable increase in fluorescence lifetime (170 ps) of TMA-DPH in presence of high peptide concentration (10 µM) in POPC/POPG/Chol (60/20/20 mol%) membranes. This result suggested that the oligomer displaces water molecules (highly polar) from the interfacial region of the membrane, thereby enhancing the lifetime of TMA-DPH in the membrane in presence of 20 mol% of cholesterol.
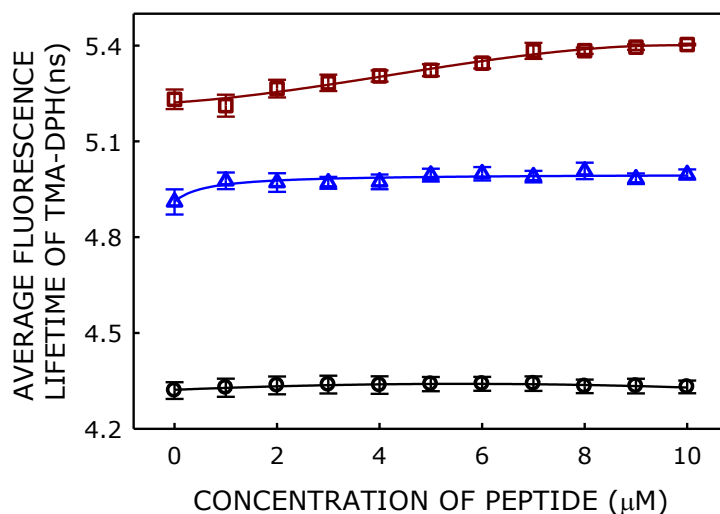

Figure 6. Plot of mean fluorescence lifetime of TMA-DPH in varying concentration of SARS-CoV fusion peptide in in POPC/POPG (80/20 mol%) (black, o), POPC/POPG/Chol (70/20/10 mol%) (blue, Δ) and POPC/POPG/Chol (60/20/20 mol%) (red, □) membranes. All experiments were carried out in a 10 mM phosphate buffer of pH 7.4 at 25 ºC. The concentration of lipid and TMA-DPH were kept constant at 200 µM and 1 µM, respectively. The emission was monitored at 428 nm by exciting at 338 nm. See the Materials and Methods section for more details.

Both Monomer and Oligomer Showed Similar Secondary Structures. The SARS-CoV fusion peptide had been already shown to assume majorly α-helical conformation in DPC micelles.[26] However, at several instances, an alteration of secondary structure in lipid membranes has been reported.[24] Moreover, the secondary structure has also been shown to depend on lipid composition of the membrane. The tryptophan fluorescence anisotropy measurements clearly showed the SARS-CoV fusion peptide to undergo composition-dependent oligomerization. Therefore, it is important to know the secondary structure of both monomeric and oligomeric species in the membrane milieu. We carried out far-UV circular dichroism (CD) spectroscopy to evaluate the secondary structure of the peptide in different membranes. We have used low lipid concentration (100 µM) to avoid scattering from the vesicular systems. The mean molar ellipticity per residue of SARS-CoV fusion peptide, in three different membranes, is shown in Figure 7 in a lipid-to-peptide ratio of 15. The peptide was monomeric in POPC/POPG membranes and oligomeric in POPC/POPG/Chol membranes with a lipid-to-peptide ratio of 15 (see Figure 2). Interestingly, there was no significant difference in CD spectra of the fusion peptide in three different membranes, except for the absolute value of mean residue ellipticity per residue being higher in the membrane having 10 mol% cholesterol. The CD spectra were analyzed using Dichroweb software[32-33] to evaluate the secondary structural components of SARS fusion peptide in three different membranes. Analysis showed the peptide to be mainly unstructured (approximately 70%), with nearly 20% β-sheet and less than 10% α-helical conformation in the membrane with and without cholesterol, respectively. Therefore, CD spectroscopy results demonstrated both monomeric and oligomeric species to have similar secondary structures.
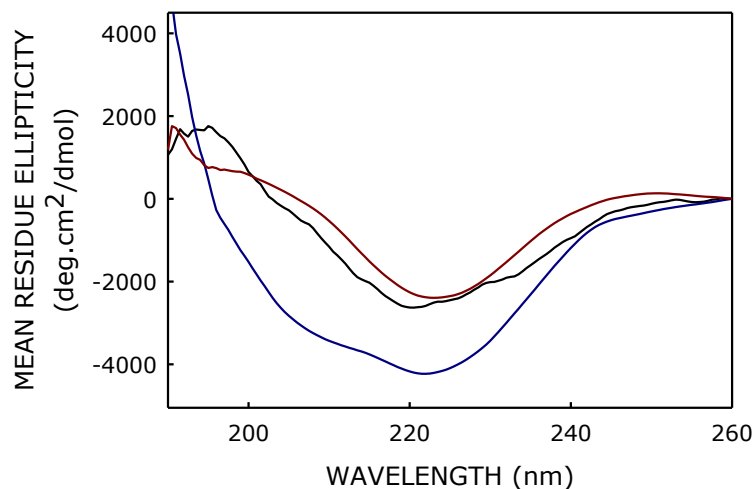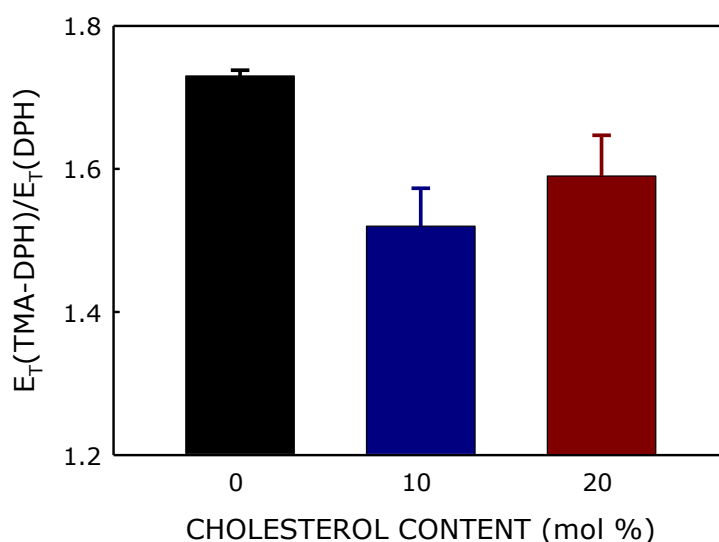
Figure 7. Plot of mean residue ellipticity of SARS-CoV fusion peptide in POPC/POPG (80/20,

mol%) (black), POPC/POPG/CH (70/20/10, mol%) (blue) and POPC/POPG/CH (60/20/20, mol%)

(red) membranes. The lipid concentration was kept constant at 100 µM and peptide concentration

was fixed at 7.5 µM. All the measurements were carried out in 5 mM phosphate buffer of pH 7.4 at

25 ℃ temperature. The CD measurements are average of at least three independent measurements.

See the Materials and Methods section for more details.

Cholesterol Altered Penetration Depth of the SARS-CoV Fusion Peptide. Penetration

depth of the peptide was evaluated by measuring FRET efficiency of tryptophan with TMA-DPH

and DPH, as discussed in the Materials and methods section, and the results are shown in Figure 8.

The location of tryptophan could be determined from the ratio of FRET efficiency of tryptophan

with TMA-DPH to that with DPH, E_T(TMA-DPH)/E_T(DPH).[46]   High value of the ratio was

indicative of proximity of tryptophan to TMA-DPH (shallow penetration), whereas a low value

would suggest its deeper penetration. Our results showed the ratio to be high in POPC/POPG (80/20

mol%) membranes, and significantly reduced in POPC/POPG/Chol (70/20/10 mol%) memrbanes.

The FRET ratio increased further in POPC/POPG/Chol (60/20/20 mol%) membranes.   Taken

21

together, penetration depth results suggested the tryptophan to be located in the interfacial region, close to TMA-DPH in POPC/POPG (80/20 mol%) membranes, a deeper penetration in POPC/POPG/Chol (70/20/10 mol%) membranes, and again in the interfacial region in POPC/POPG/Chol (60/20/20 mol%) membranes. Taken together, deeper penetration of the peptide might be responsible for increased DPH anisotropy in POPC/POPG/Chol (70/20/10 mol%) membranes, whereas interfacial location of the peptide migth lead to disruption of interfacial order of the POPC/POPG/Chol (60/20/20 mol%) membranes.

Figure 8. Plot of FRET efficiency of tryptophan with TMA-DPH and DPH, E_T(TMA-DPH)/E_T(DPH), of SARS fusion peptide in POPC/POPG (80/20, mol%) (black), POPC/POPG/Chol (70/20/10, mol%) (blue) and POPC/POPG/Chol (60/20/20, mol%) (red) membranes. The lipid concentration was kept constant at 200 µM and peptide concentration was fixed at 2 µM. The TMA-DPH and DPH concentrations are kept constant at 2 µM. All the measurements were carried out in 10 mM phosphate buffer of pH 7.4 at 25 ºC temperature. All measurements are average of at least three independent measurements. See the Materials and Methods section for more details.

DISCUSSION

The most important step in viral entry into the host cell is the fusion between viral membrane and host cell or organelle membranes. Generally, the N-terminal sequence of fusion protein, with a distribution of hydrophobic and hydrophilic amino acids, is the fusion peptide that facilitates membrane fusion. SARS fusion peptide, a 19-amino acid stretch from SARS-CoV, is instrumental in promoting fusion between SARS virus and host cells. In addition to the peptide, membrane composition plays an important role in promoting membrane fusion. To understand the underlying reason, we have used arrays of spectroscopic methods to measure the peptide conformation and its effect on organization and dynamics of POPC/POPG membranes with varying compositions. We have maintained 20 mol% of POPG in our measurements, since SARS-CoV fusion peptide has been shown to predominantly bind to membranes with negatively charged phospholipids.[3] Interestingly, the fusion peptide of SARS-CoV demonstrated higher binding affinity to cholesterol containing membranes. The binding K_d was approximately 12-fold smaller in POPC/POPG/Chol (60/20/20 mol%) membranes than in POPC/POPG (80/20 mol%) membranes. We observed tryptophan fluorescence intensity to increase with binding of the peptide in POPC/POPG (80/20 mol%) and POPC/POPG/Chol (70/20/10 mol%) membranes, and decrease after binding to POPC/POPG/Chol (60/20/20 mol%) membranes. The reduction of fluorescence intensity might be attributed to either conformational change or oligomerization of the peptide in the membrane containing 20 mol% of cholesterol, which might have exposed the tryptophan to a quenching amino acid, like phenylalanine. This result provided crucial information regarding the differential behavior of SARS-CoV fusion peptide in the 20 mol% cholesterol-containing membranes. Tryptophan anisotropy measurement in different membranes, as a function of peptide concentration, clearly showed the peptide to oligomerize in the cholesterol-containing membrane, the oligomerization being initiated at very low

peptide concentrations in the membrane containing 20 mol% cholesterol. Anisotropy results corroborated with the decrease of fluorescence intensity observed in the binding experiment, and seconded the claim of oligomerization of SARS-CoV fusion peptide in the membrane containing 20 mol% cholesterol. Oligomerization of the fusion peptide has tremendous significance in membrane fusion. It has been postulated to promote six-helix bundle formation, which provides the requisite energy to overcome the activation barrier for membrane fusion.[47] However, very little information is available regarding the oligomerization of fusion peptide, since most of the oligomeric structures have been solved with the fusion protein without fusion peptide and transmembrane domain.[42, 44] To the best of our knowledge, this is the first report that demonstrated the oligomerization of wild type sequence of SARS-CoV fusion peptide in membranes, and elucidated the strong dependence of oligomerization on the abundance of membrane cholesterol.

We further monitored the effect of SARS-CoV fusion peptide on the organization and dynamics of membranes with varying lipid compositions. Anisotropy measurement of DPH and TMA-DPH in membranes provided information about depth-dependent ordering of the membrane. The fusion peptide was found to have maximum effect on hydrophobic ordering (DPH anisotropy) in a membrane containing 10 mol% cholesterol. The peptide-mediated enhancement of order in the hydrophobic tail region might be attributed to the deeper penetration of the peptide into the membrane, thereby enhancing the packing of hydrophobic tails. Therefore, our result indicated the peptide to possibly be penetrating deeper into the 10 mol% cholesterol-containing membrane compared to the rest. However, the peptide did not change polarity of the hydrophobic region of the membrane. We monitored the ordering of the interfacial region of the membrane by exploiting fluorescence anisotropy measurements of TMA-DPH. Interestingly, the fusion peptide disrupted the interfacial order of POPC/POPG/Chol (60/20/20 mol%) membranes, where the peptide mainly

existed as an oligomer. This result implied the oligomeric form to be mainly located at the interfacial region, possibly disrupting the headgroup-headgroup and/or headgroup-water interaction, resulting in decreased interfacial order. The partial increase in fluorescence lifetime, at higher peptide concentration, in the membrane containing 20 mol% cholesterol supported the assumption of disruption of headgroup-headgroup and/or headgroup-water interaction, thereby effectively reducing interfacial polarity.

Circular dichroism spectroscopy results showed the peptide to assume mainly unstructured conformation with approximately 20% β-sheet and 10% α-helical conformation in the three membranes, thus suggesting the differential impact of the peptide in three different membranes do not arise from the conformational change of the peptide. Therefore, oligomerization and effect of lipid composition on lipid-peptide interaction could be a plausible reason for the differential effect of the peptide on organization and dynamics of the membrane. Difference in lipid composition provides different environments for peptide solubilization,[23] and accordingly, the effect of peptide penetration produces differential impact on membrane dynamics and organization. Our result further demonstrated the secondary structure to be strongly dependent on the environment; while the peptide is majorly α-helical in DPC micelles, it loses the α-helical conformation in lipid vesicles. Measurement of FRET efficiency of tryptophan with DPH and TMA-DPH provided information about the location of tryptophan in the membrane. The tryptophan is located more in the hydrophobic region of the membrane containing 10 mol% cholesterol. Our results corroborated with the observed change in peptide-induced hydrophobic order in POPC/POPG/Chol (70/20/10 mol%) membranes. The tryptophan was found to be located more toward the headgroup (close to TMA-DPH) in the membrane containing either no cholesterol or 20 mol% cholesterol. While the peptide is monomeric in POPC/POPG (80/20 mol%) membranes, it is oligomeric in membranes containing

20 mol% of cholesterol. TMA-DPH anisotropy was significantly affected by the peptide in the membrane containing 20 mol% cholesterol. Taken together, our result demonstrated the oligomer of SARS-CoV fusion peptide to have significant membrane disrupting ability compared to its monomeric counterpart. In summary, our results provided novel insight into the interaction of SARS-CoV fusion peptide with membranes containing different amounts of cholesterol, and could have important implications in membrane fusion.

ACKNOWLEDGMENTS

REFERENCES

1.   Stadler, K.; Masignani, V.; Eickmann, M.; Becker, S.; Abrignani, S.; Klenk, H. D.; Rappuoli,

R. SARS--beginning to understand a new virus. *Nat. Rev. Microbiol.* **2003**, *1*, 209-18.

2.   Hofmann, H.; Pohlmann, S. Cellular entry of the SARS coronavirus. *Trends Microbiol.* **2004**,

12, 466-72.

3.   Guillen, J.; de Almeida, R. F.; Prieto, M.; Villalain, J. Structural and dynamic

characterization of the interaction of the putative fusion peptide of the S2 SARS-CoV virus

protein with lipid membranes. *J. Phys. Chem. B* **2008**, *112*, 6997-7007.

4.   Gallagher, T. M.; Buchmeier, M. J. Coronavirus spike proteins in viral entry and

pathogenesis. *Virology* **2001**, *279*, 371-4.

5.   Jeffers, S. A.; Tusell, S. M.; Gillim-Ross, L.; Hemmila, E. M.; Achenbach, J. E.; Babcock,

G. J.; Thomas, W. D., Jr.; Thackray, L. B.; Young, M. D.; Mason, R. J.; et al. CD209L (L-

SIGN) is a receptor for severe acute respiratory syndrome coronavirus. *Proc. Natl. Acad. Sci.*

U. S. A. **2004**, *101*, 15748-53.

6.   Li, W.; Moore, M. J.; Vasilieva, N.; Sui, J.; Wong, S. K.; Berne, M. A.; Somasundaran, M.;

Sullivan, J. L.; Luzuriaga, K.; Greenough, T. C.; et al. Angiotensin-converting enzyme 2 is

a functional receptor for the SARS coronavirus. *Nature* **2003**, *426*, 450-4.

7.   Beniac, D. R.; deVarennes, S. L.; Andonov, A.; He, R.; Booth, T. F. Conformational

reorganization of the SARS coronavirus spike following receptor binding: implications for

membrane fusion. *PLoS One* **2007**, *2*, e1082.

8.   Taguchi, F.; Shimazaki, Y. K. Functional analysis of an epitope in the S2 subunit of the

murine coronavirus spike protein: involvement in fusion activity. *J. Gen. Virol.* **2000**, *81*,

2867-71.

27

9. Cavanagh, D.; Davis, P. J. Coronavirus IBV: removal of spike glycopolypeptide S1 by urea abolishes infectivity and haemagglutination but not attachment to cells. *J. Gen. Virol.* **1986**, *67*, 1443-8.

10. Taguchi, F. The S2 subunit of the murine coronavirus spike protein is not involved in receptor binding. *J. Virol.* **1995**, *69*, 7260-3.

11. Tripet, B.; Howard, M. W.; Jobling, M.; Holmes, R. K.; Holmes, K. V.; Hodges, R. S. Structural characterization of the SARS-coronavirus spike S fusion protein core. *J. Biol. Chem.* **2004**, *279*, 20836-49.

12. Liu, S.; Xiao, G.; Chen, Y.; He, Y.; Niu, J.; Escalante, C. R.; Xiong, H.; Farmar, J.; Debnath, A. K.; Tien, P.; Jiang, S. Interaction between heptad repeat 1 and 2 regions in spike protein of SARS-associated coronavirus: implications for virus fusogenic mechanism and identification of fusion inhibitors. *Lancet* **2004**, *363*, 938-47.

13. Bosch, B. J.; Martina, B. E.; Van Der Zee, R.; Lepault, J.; Haijema, B. J.; Versluis, C.; Heck, A. J.; De Groot, R.; Osterhaus, A. D.; Rottier, P. J. Severe acute respiratory syndrome coronavirus (SARS-CoV) infection inhibition using spike protein heptad repeat-derived peptides. *Proc. Natl. Acad. Sci. U. S. A.* **2004**, *101*, 8455-60.

14. Bosch, B. J.; van der Zee, R.; de Haan, C. A.; Rottier, P. J. The coronavirus spike protein is a class I virus fusion protein: structural and functional characterization of the fusion core complex. *J. Virol.* **2003**, *77*, 8801-11.

15. Hakansson-McReynolds, S.; Jiang, S.; Rong, L.; Caffrey, M. Solution structure of the severe acute respiratory syndrome-coronavirus heptad repeat 2 domain in the prefusion state. *J. Biol. Chem.* **2006**, *281*, 11965-71.

16. Deng, Y.; Liu, J.; Zheng, Q.; Yong, W.; Lu, M. Structures and polymorphic interactions of two heptad-repeat regions of the SARS virus S2 protein. *Structure* **2006**, *14*, 889-99.

17. Supekar, V. M.; Bruckmann, C.; Ingallinella, P.; Bianchi, E.; Pessi, A.; Carfí, A. Structure of a proteolytically resistant core from the severe acute respiratory syndrome coronavirus S2 fusion protein. *Proc. Natl. Acad. Sci. U. S. A.* **2004**, *101*, 17958-17963.

18. Xu, Y.; Lou, Z.; Liu, Y.; Pang, H.; Tien, P.; Gao, G. F.; Rao, Z. Crystal structure of severe acute respiratory syndrome coronavirus spike protein fusion core. *J. Biol. Chem.* **2004**, *279*, 49414-9.

19. Pattnaik, G. P.; Meher, G.; Chakraborty, H. Exploring the Mechanism of Viral Peptide-Induced Membrane Fusion. *Adv. Exp. Med. Biol.* **2018**, *1112*, 69-78.

20. Simmons, G.; Gosalia, D. N.; Rennekamp, A. J.; Reeves, J. D.; Diamond, S. L.; Bates, P. Inhibitors of cathepsin L prevent severe acute respiratory syndrome coronavirus entry. *Proc. Natl. Acad. Sci. U. S. A.* **2005**, *102*, 11876-81.

21. Wang, H.; Yang, P.; Liu, K.; Guo, F.; Zhang, Y.; Zhang, G.; Jiang, C. SARS coronavirus entry into host cells through a novel clathrin- and caveolae-independent endocytic pathway. *Cell Res.* **2008**, *18*, 290-301.

22. Guillen, J.; De Almeida, R. F.; Prieto, M.; Villalain, J. Interaction of a peptide corresponding to the loop domain of the S2 SARS-CoV virus protein with model membranes. *Mol. Membr. Biol.* **2009**, *26*, 236-48.

23. Meher, G.; Sinha, S.; Pattnaik, G. P.; Ghosh Dastidar, S.; Chakraborty, H. Cholesterol Modulates Membrane Properties and the Interaction of gp41 Fusion Peptide To Promote Membrane Fusion. *J. Phys. Chem. B* **2019**, *123*, 7113-7122.

24. Meher, G.; Chakraborty, H. Membrane Composition Modulates Fusion by Altering Membrane Properties and Fusion Peptide Structure. *J. Membr. Biol.* **2019**.

25. Guillen, J.; Kinnunen, P. K.; Villalain, J. Membrane insertion of the three main membranotropic sequences from SARS-CoV S2 glycoprotein. *Biochim. Biophys. Acta* **2008**, *1778*, 2765-2774.

26. Lai, A. L.; Moorthy, A. E.; Li, Y.; Tamm, L. K. Fusion activity of HIV gp41 fusion domain is related to its secondary structure and depth of membrane insertion in a cholesterol-dependent fashion. *J. Mol. Biol.* **2012**, *418*, 3-15.

27. Mahajan, M.; Bhattacharjya, S. NMR structures and localization of the potential fusion peptides and the pre-transmembrane region of SARS-CoV: Implications in membrane fusion. *Biochim. Biophys. Acta* **2015**, *1848*, 721-30.

28. Mahajan, M.; Chatterjee, D.; Bhuvaneswari, K.; Pillay, S.; Bhattacharjya, S. NMR structure and localization of a large fragment of the SARS-CoV fusion protein: Implications in viral cell fusion. *Biochim. Biophys. Acta* **2018**, *1860*, 407-415.

29. Sainz, B., Jr.; Rausch, J. M.; Gallaher, W. R.; Garry, R. F.; Wimley, W. C. Identification and characterization of the putative fusion peptide of the severe acute respiratory syndrome-associated coronavirus spike protein. *J. Virol.* **2005**, *79*, 7195-206.

30. MacDonald, R. C.; MacDonald, R. I.; Menco, B. P.; Takeshita, K.; Subbarao, N. K.; Hu, L. R. Small-volume extrusion apparatus for preparation of large, unilamellar vesicles. *Biochim. Biophys. Acta* **1991**, *1061*, 297-303.

31. Meher, G.; Chakraborty, H. Influence of Eugenol on the Organization and Dynamics of Lipid Membranes: A Phase-Dependent Study. *Langmuir* **2018**, *34*, 2344-2351.

32. Lakowicz, J. R. Principles of Fluorescence Spectroscopy. *Springer* **2006**, *3rd Edition*.

33.   Whitmore, L.; Wallace, B. A. Protein secondary structure analyses from circular dichroism spectroscopy: methods and reference databases. *Biopolymers* **2008**, *89*, 392-400.

34.   Whitmore, L.; Wallace, B. A. DICHROWEB, an online server for protein secondary structure analyses from circular dichroism spectroscopic data. *Nucleic Acids Res.* **2004**, *32*, W668-73.

35.   Kaiser, R. D.; London, E. Location of diphenylhexatriene (DPH) and its derivatives within membranes: comparison of different fluorescence quenching analyses of membrane depth. *Biochemistry* **1998**, *37*, 8180-90.

36.   Wu, P.; Brand, L. Resonance energy transfer: methods and applications. *Anal. Biochem.* **1994**, *218*, 1-13.

37.   Pattnaik, G. P.; Chakraborty, H. Coronin 1 derived tryptophan-aspartic acid containing peptides inhibit membrane fusion. *Chem. Phys. Lipids* **2018**, *217*, 35-42.

38.   Koppaka, V.; Lentz, B. R. Binding of bovine factor Va to phosphatidylcholine membranes. *Biophys. J.* **1996**, *70*, 2930-7.

39.   Meher, G.; Chakraborty, H. Organization and dynamics of Trp14 of hemagglutinin fusion peptide in membrane mimetic environment. *Chem. Phys. Lipids* **2017**, *205*, 48-54.

40.   Ganguly, S.; Clayton, A. H.; Chattopadhyay, A. Organization of higher-order oligomers of the serotonin(1)(A) receptor explored utilizing homo-FRET in live cells. *Biophys. J.* **2011**, *100*, 361-8.

41.   Chakraborty, H.; Chattopadhyay, A. Excitements and challenges in GPCR oligomerization: molecular insight from FRET. *ACS Chem. Neurosci.* **2015**, *6*, 199-206.

42.   Jameson, D. A. Introduction to Fluorescence. *CRC Press* **2014**.

43.   Chan, D. C.; Fass, D.; Berger, J. M.; Kim, P. S. Core structure of gp41 from the HIV envelope glycoprotein. *Cell* **1997**, *89*, 263-73.

44.   Qiang, W.; Sun, Y.; Weliky, D. P. A strong correlation between fusogenicity and membrane insertion depth of the HIV fusion peptide. *Proc. Natl. Acad. Sci. U. S. A.* **2009**, *106,* 15314-9.

45.   Xiao, X.; Feng, Y.; Chakraborti, S.; Dimitrov, D. S. Oligomerization of the SARS-CoV S glycoprotein: dimerization of the N-terminus and trimerization of the ectodomain. *Biochem. Biophys. Res. Commun.* **2004**, *322*, 93-9.

46.   Pattnaik, G. P.; Chakraborty, H. Cholesterol Alters the Inhibitory Efficiency of Peptide-based Membrane Fusion Inhibitor. *Biochim. Biophys. Acta (Biomembranes)* **2019**, *1861*, 183056.

47.   Kielian, M. Mechanisms of Virus Membrane Fusion Proteins. *Annu. Rev. Virol.* **2014**, *1*, 171-89.

<u>FOR TABLE OF CONTENT ONLY</u>